Crystallization Behavior of Mannitol in Frozen Aqueous Solutions

Raghu K. Cavatur,[1,2] N. Murti Vemuri,[3] Abira Pyne,[1,4] Zofia Chrzan,[3] David Toledo-Velasquez,[5] and Raj Suryanarayanan[1,6]

Received February 19, 2002; accepted February 28, 2002

Purpose. To study the effect of cooling rate, the influence of phosphate buffers and polyvinylpyrrolidone (PVP) on the crystallization behavior of mannitol in frozen aqueous solutions.

Methods. Low-temperature differential scanning calorimetry and powder X-ray diffractometry were used to characterize the frozen solutions.

Results. Rapid cooling (20°C/min) inhibited mannitol crystallization, whereas at slower cooling rates (10°C and 5°C/min) partial crystallization was observed. The amorphous freeze-concentrate was characterized by two glass transitions at –32°C and –25°C. When the frozen solutions were heated past the two glass transition temperatures, the solute crystallized as mannitol hydrate. An increase in the concentration of PVP increased the induction time for the crystallization of mannitol hydrate. At concentrations of ≥100 mM, the buffer salts significantly inhibited mannitol crystallization.

Conclusions. The crystallization behavior of mannitol in frozen solutions was influenced by the cooling rate and the presence of phosphate buffers and PVP.

KEY WORDS: mannitol; frozen; differential scanning calorimetry; X-ray powder diffractometry.

INTRODUCTION

The development of parenteral protein formulations poses some unique challenges. The limited stability of proteins in aqueous solutions often precludes liquid formulations. Of the numerous stabilization techniques available, freeze-drying has been established as the dry-state stabilization method of choice for many labile pharmaceuticals. However, during the freeze-drying process, the protein molecules encounter freezing and drying stresses, which can result in their denaturation (1,2). Hence, during the design of a freeze-dried formulation, several process and formulation factors have to be optimized so as to ensure that the active ingredient does not undergo irreversible physical and chemical changes and also to assure long-term stability during storage (3).

Of the different additives that are used in a freeze-dried formulation, lyoprotectants play an active role in protecting proteins from denaturation (3). It has been postulated that lyoprotectants form hydrogen bonds with proteins, acting as replacement for the hydration shell, and hence maintain the native conformation of the protein (4). Lyoprotectants have been found to be maximally efficient when they are present in the amorphous state (4). The crystallization of the lyoprotectant during lyophilization or during storage results in the loss of lyoprotectant activity and in subsequent destabilization of the protein molecule (5).

Mannitol is widely used as a bulking agent in freeze-dried formulations. Though mannitol is inert and has good cake-supporting properties, it crystallizes readily during freeze-drying, and therefore does not possess any lyoprotectant activity. Interestingly, phosphate buffer salts inhibited the crystallization of mannitol during freeze-drying, resulting in improved lyoprotectant activity (5). Therefore, mannitol possibly can be used as a lyoprotectant by inhibiting its crystallization during freeze-drying and subsequent storage. Additionally, various process factors were shown to have an influence on the solid state of mannitol in the freeze-dried formulations (6).

It is a common practice to perform detailed characterization studies of the ingredients of a dosage form and also the final freeze-dried product. The physical state of the solute in a frozen system is often not the subject of detailed investigations. Because the final physical state of the freeze-dried product is influenced by the physical state of the solute in a frozen solution, a more rational approach is to perform characterization studies during various stages of the freeze-drying process. This is particularly important in the case of mannitol, because in addition to several polymorphic forms of anhydrous mannitol, the existence of mannitol hydrate and an amorphous form of mannitol have been reported (7,8). Such characterization studies are helpful in the design of an optimum formulation assuring long-term stability of the therapeutic protein.

The characterization of frozen aqueous solutions of mannitol was the first step in this process. This article reports the effect of process factors as well as formulation factors on the physical state of mannitol in frozen aqueous solutions. The effect of cooling rate on the crystallization of mannitol and the transitions during heating of frozen aqueous solutions of mannitol were first investigated. The influence of polyvinylpyrrolidone (PVP; a macromolecular additive that is also known to serve as a crystallization inhibitor) and phosphate buffer salts on the crystallization of mannitol in frozen aqueous solutions was evaluated next. Differential scanning calorimetry (DSC) and powder X-ray diffractometry (XRD) were the instrumental techniques used to characterize the systems.

MATERIALS AND METHODS

Materials

Mannitol ($C_6H_{14}O_6$; Sigma, St. Louis, Missouri), monobasic potassium phosphate (Sigma), dibasic potassium phosphate (Sigma), and PVP (28–32 K; Sigma) were used as received.

Methods

DSC

A differential scanning calorimeter equipped with a liquid nitrogen cooling accessory (Model 220C, Seiko, Tokyo, Japan) was used. The DSC cell was calibrated using indium

[1] Department of Pharmaceutics, 308 Harvard Street, S.E., University of Minnesota, Minneapolis, Minnesota 55455.
[2] Current address: Aventis Pharmaceuticals, Bridgewater, New Jersey.
[3] Aventis Pharmaceuticals, Bridgewater, New Jersey.
[4] Current address: Eli Lilly and Company, Indianapolis, Indiana.
[5] Merck and Company, West Point, Pennsylvania.
[6] To whom correspondence should be addressed. (email: surya001@tc.umn.edu)

0724-8741/02/0600-0894/0 © 2002 Plenum Publishing Corporation

and distilled water. Between 2 and 6 mg of the sample solution was weighed into an aluminum pan, the pan was sealed nonhermetically, and the sample solutions were cooled from room temperature to –50°C at cooling rates of 20°C, 10°C, or 5°C/min. The samples were held at –50°C for 5 min before being heated to 20°C at a heating rate of either 10°C or 1°C/min. The samples were purged with nitrogen during both the heating and cooling phases.

Similarly, solutions of mannitol (10% w/w) also were subjected to DSC studies in the presence either of potassium phosphate buffer salts (pH 7.0) or PVP. The experimental conditions and the additive concentrations are presented in the Results and Discussion section.

Low-Temperature Powder XRD

An X-ray powder diffractometer (model XDS 2000, Scintag, Cupertino, California) with a variable temperature stage (Micristar, model 828D, R.G. Hansen & Associates, Santa Barbara, California; working temperature range of –190°C to +300°C) was used. About 100 mg of the solution was filled into a copper sample holder. The solutions were cooled from 10°C to –50°C at three different cooling rates of 20°C, 10°C, and 5°C/min. The samples were heated at 5°C/min, to –3°C, and XRD patterns were obtained at –50, –35, –25, –10 and –3°C. Solutions of mannitol (10% w/w) in the presence of potassium phosphate salts or PVP were cooled from 10°C to –50°C at either 5°C or 1°C/min. These frozen solutions were then heated to –3°C at 5°C/min, and the XRD patterns were obtained as a function of temperature at –50°C, –35°C, –25°C, –10°C, and –3°C. For all the above solutions, the angular range of XRD analysis was 8°2θ to 40°2θ. Diffraction patterns were obtained under the continuous-scan mode with a chopper increment of 0.05°2θ and at a scanning rate of 2°2θ/min.

RESULTS AND DISCUSSION

Characterization of "As Is" Mannitol

The "as is" mannitol was characterized by XRD and DSC. The XRD pattern of mannitol matched that of the anhydrous β-polymorph (7). When heated in a crimped pan in the DSC, mannitol melted at ~165°C.

Characterization of Frozen Aqueous Solutions of Mannitol

Transitions during Cooling

The DSC curve of an aqueous mannitol solution (15% w/v), cooled from 20°C to –50°C at 20°C/min, revealed an exotherm at ~ –24°C that was attributed to the crystallization of ice. Because no other exotherms were observed, it was concluded that mannitol did not crystallize and remained as an amorphous freeze-concentrate. At cooling rates of 10°C and 5°C/min, the crystallization of ice was followed by a second exotherm. This was attributed to the crystallization of mannitol, although the extent of its crystallization is unknown. Qualitatively similar results were obtained when mannitol solutions of lower concentrations (5–12.5% w/w) were cooled either at 5°C or 10°C/min.

In an effort to obtain quantitative information, the enthalpy of crystallization obtained from the second exotherm were plotted as a function of mannitol concentration in Fig. 1.

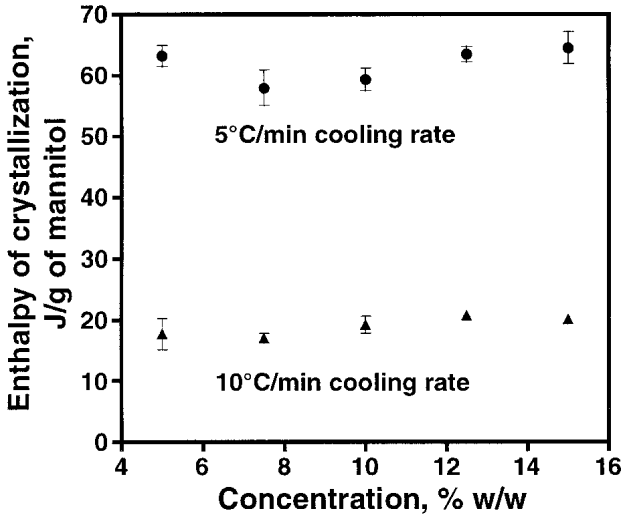

Fig. 1. Enthalpy of mannitol crystallization as a function of its concentration at cooling rates of 5°C and 10°C/min. Values are given as mean ± SD (n = 3).

At each concentration, the observed enthalpy values were normalized for the amount of mannitol present. (It is well-known that there will be unfrozen water associated with amorphous mannitol; when there is crystallization, the observed enthalpy is due to the crystallization of mannitol as well as to the unfrozen water.) The plot reveals two facts. (1) The enthalpy values were independent of the initial mannitol concentration. In other words, for a fixed cooling rate, the fraction of mannitol (and the associated water) crystallizing from solution was constant and was concentration-independent. Moreover, the solid state of mannitol crystallizing from solution seemed to be independent of the initial mannitol concentration in solution. (2) The observed enthalpy of crystallization was dependent on the cooling rate. A decrease in cooling rate caused a much larger fraction of the mannitol along with the associated unfrozen water to crystallize from solution.

Low-temperature XRD of mannitol solutions revealed that cooling at 20°C/min resulted only in the crystallization of ice (data not shown). Similarly, at cooling rates of 10°C/min (data not shown) and 5°C/min (Fig. 2), no XRD peaks attributable to mannitol were observed. All the observed peaks were due to ice. However, the DSC data suggest that at cooling rates of 10°C and 5°C/min, the crystallization of mannitol had occurred. It is possible that the amount of crystallized mannitol is below the detection limit of XRD. This suggests that DSC is a more sensitive technique for the detection of crystallizing mannitol. However, it must be recognized that the DSC and XRD techniques have pronounced differences both in sample size and sample geometry. An added complication is that the there are differences in the temperature program and therefore the thermal history of the sample. The observed differences in results between DSC and XRD may be attributed to these factors.

Effect of Potassium Phosphate Buffer Salts and PVP on Mannitol Crystallization during Cooling

Buffer salts are known to inhibit the crystallization of solutes in frozen solutions. Specifically, the presence of buffer

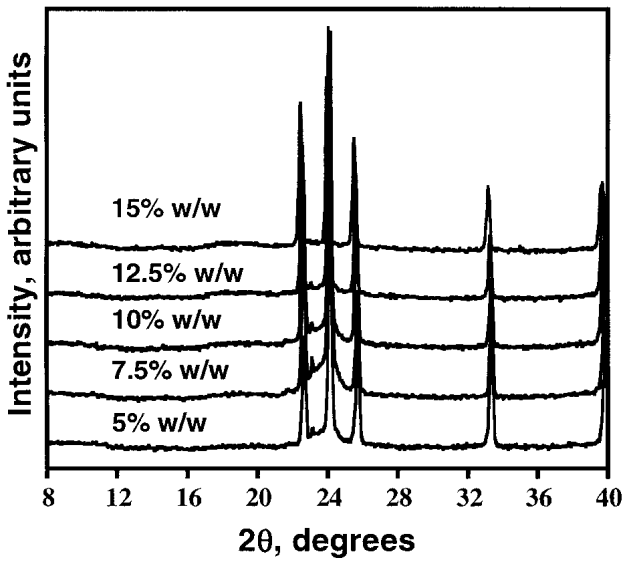

Fig. 2. XRD patterns of mannitol solutions cooled from room temperature to –50°C at 5°C/min. All the peaks are attributable to hexagonal ice.

salts has been shown to inhibit the crystallization of mannitol in freeze-dried solids (5). In our experiments, the mannitol concentration was fixed at 10% (w/w), whereas the buffer salt concentration was varied. The influence of three buffer salt concentrations were examined (50, 100, and 150 mM). These solutions were cooled at either 1°C or 5°C/min. The observed exotherms were attributed to the crystallization of ice, followed by mannitol. In the concentration range used and at the cooling rates employed, both the buffer salts are expected to remain amorphous (9). The enthalpy of mannitol crystallization, which was calculated from the second exotherm, is presented in Table 1.

The solid state of crystalline mannitol in the presence of buffer salts was characterized by low-temperature XRD. Peaks in the XRD pattern, other than those due to hexagonal ice, were attributed to crystalline mannitol hydrate. The stoichiometric water content of mannitol hydrate is not known (10,11). Table 1 contains the integrated intensities and the full width at half maximum (FWHM) of a characteristic peak of mannitol hydrate which occurs at 9.5°2θ.

Based on the heats of crystallization values, it can be inferred that the crystallization behavior of mannitol during cooling was influenced by the buffer salts. At all buffer salt concentrations, mannitol crystallization was inhibited when the cooling rate was 5°C/min. However, at a slower cooling rate of 1°C/min, mannitol crystallization was observed only at a buffer salt concentration of 50 mM.

The low-temperature XRD results corroborate the DSC results. At a cooling rate of 5°C/min, there was no evidence of mannitol crystallization. The integrated counts (~9000) were attributed to the background in the XRD pattern. However, at a cooling rate of 1°C/min, the characteristic XRD peaks of mannitol hydrate (10,11) were observed when the buffer salt concentration was 50 mM (Table 1). Mannitol crystallization was not evident at cooling rates of 1°C/min and at buffer concentrations of 100 and 150 mM. We had earlier observed crystallization of mannitol hydrate when aqueous solutions were cooled at 1°C/min. At a buffer concentration of 50 mM, although there was a decrease in the integrated counts, only a small change in the peak width (measured as the FWHM) was observed, indicating that the crystallinity of mannitol was unaffected by the buffer salts (Table 1). Sodium phosphate buffer salts were shown to inhibit the crystallization of glycine in frozen solutions, possibly by altering the crystallization kinetics (12). A similar mechanism can be postulated for the inhibition of mannitol crystallization by potassium phosphate buffer salts. Therefore, the buffer salts possibly influence the nucleation rate, and the magnitude of this effect seems to be dependent on their concentration in solution and the cooling rates.

The effect of PVP on the crystallization of mannitol was investigated next. As before, the mannitol concentration was fixed at 10% (w/w) and the PVP concentration was varied between 0.45 and 4.5% (w/w). The solutions were cooled either at 1 or at 5°C/min. The observed exotherms were attributed to the crystallization of ice, followed by that of mannitol hydrate. The enthalpy of mannitol crystallization, calculated from the second exotherm, is presented in Table 2. At a cooling rate of 5°C/min, PVP exhibited a concentration-dependent inhibition of mannitol crystallization. This conclusion was based on the progressive decrease in enthalpy of mannitol crystallization as a function of PVP concentration (Table 2). The complete inhibition of mannitol crystallization occurred at a PVP concentration of 4.5% (w/w). At a cooling rate of 1°C/min, there seems to be no inhibition in mannitol crystallization up to a PVP concentration of 0.9% (w/w) (Table 2). At higher PVP concentrations, again, a concentra-

Table I. Effect of Potassium Phosphate Buffer Salt Concentration on the Enthalpy of Crystallization of Mannitol, and on the Intensity and FWHM of the 9.1°2θ Peak of Mannitol Hydrate

	Mannitol					
Concentration of buffer salts (mM)	Normalized heat of crystallization (J/g) Cooling rate (°C/min)		Integrated intensity (counts) Cooling rate (°C/min)		(FWHM (°) Cooling rate (°C/min)	
	5	1	5	1	5	1
0	–63.0	–71.0	[a]	13,268		0.148
50	No crystallization	–53.0	[a]	11,341		0.165
100	No crystallization	No crystallization	[a]	[a]		
150	No crystallization	No crystallization	[a]	[a]		

[a] No peak attributable to mannitol was observed in the XRD pattern at –50°C.

Table II. Effect of PVP Concentration on (i) the Enthalpy of Crystallization of Mannitol, and (ii) the Intensity of Width of the 9.1°2θ Peak of Mannitol Hydrate[a]

Concentration of PVP (% w/w)	Mannitol					
	Normalized heat of crystallization (J/g) Cooling rate (°C/min)		Integrated intensity (counts) Cooling rate (°C/min)		FWHM (°) Cooling rate (°C/min)	
	5	1	5	1	5	1
0	–63.0	–71.0	[b]	13,268		0.148
0.45	–58.0	–71.0	ND	ND	ND	ND
0.90	–53.0	–70.0	[b]	13,455		0.405
2.25	–12.0	–66.0	[b]	13,243		0.520
4.5	No crytallization	–51.0	[b]	10,017		

[a] ND, not done.
[b] No peak attributable to mannitol was observed in the XRD pattern at –50°C.

tion-dependent inhibition of mannitol crystallization was observed.

The frozen solutions also were evaluated by low-temperature powder XRD. When the solutions were cooled at 5°C/min, both in the presence and absence of PVP, there was no evidence of mannitol crystallization (Table 2). Thus, XRD seems to be a less sensitive technique than DSC. However, when the solutions were cooled at 1°C/min, peaks attributable to mannitol hydrate were observed in all the cases except at the highest PVP concentration. However, there was an increase in the width of the X-ray lines (measured as the FWHM) as a function of the PVP concentration (Table 2). Thus, an increase in the PVP concentration resulted in a decrease in the crystallinity of mannitol in frozen solutions.

PVP, a long chain polymer, is known to inhibit the crystallization of solutes from solutions by increasing the viscosity of the freeze-concentrate (13,14). A second possible mechanism of its action is through specific interaction with the solute, as has been reported in the case of indomethacin (15). From the data presented in Table 2, it is evident that the magnitude of the effect is dependent on both the PVP concentration and the cooling rate. Therefore, the likely mechanism of crystallization inhibition is an increase in the viscosity of the freeze-concentrate rather than any specific interaction between PVP and mannitol. Further investigation is necessary to develop a complete understanding of this system.

Crystallization inhibition can be achieved by a combination of process and formulation factors. Although mannitol crystallization was inhibited at high cooling rates, such rates are not feasible in commercial freeze-dryers. Alternatively, at least partial crystallization inhibition can be achieved at slower cooling rates through an additive. A potential problem with such an approach is that the additive can alter the solid state (i.e., polymorphic form) of the crystallizing solute. Although the mannitol phase crystallizing from solution did not seem to be influenced by the presence of buffer salts or PVP, low-temperature XRD revealed a concentration-dependent effect of PVP on the crystallinity of mannitol.

Although mannitol crystallization could be effectively inhibited in frozen aqueous solutions, heating these solutions may cause a number of phase transitions including solute crystallization. Because such transitions will have a bearing on the solid state of the lyophile, our next interest was to characterize the phase transitions when the frozen solutions were heated.

Transitions during the Heating of Frozen Solutions of Mannitol

Mannitol solutions were first cooled from room temperature to –50°C at 20°C/min. The solutions then were heated to 20°C at 10°C/min. The DSC heating curve revealed a number of transitions (Fig. 3). (1) The glass transition (Tg'_1) of the amorphous freeze-concentrate occurred with onset at –32°C. The glass transition temperature of anhydrous amorphous mannitol was reported to be 13.7°C (10). (2) A second glass transition (Tg'_2) occurred with onset at ~ –25°C. Although this could be construed as an endotherm, we postulate that this is a glass transition, and we have provided some supporting evidence. (3) An exotherm, attributable to the crystallization of both mannitol hydrate and the unfrozen water, occurred that was associated with the amorphous phase. (4) An overlapping eutectic and ice melting endotherm occurred. The glass transition temperature of the maximally freeze-concentrated mannitol has been reported to be ~ –30°C in the literature (6,16). Because we observed two glass transitions,

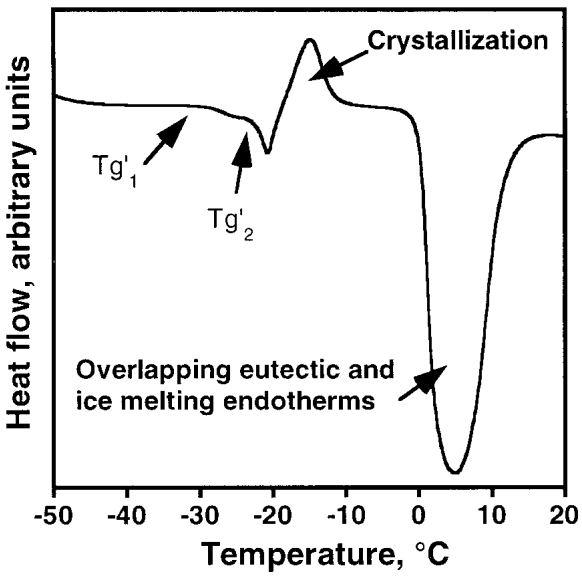

Fig. 3. The DSC curve of frozen mannitol solution (15% w/w) heated at 10°C/min from –50°C to 20°C. The inset shows an expanded view of the *y* axis over the temperature range of –50°C at 20°C/min.

we have used Tg'_1 and Tg'_2 to identify the lower and the higher transition temperatures, respectively.

To gain a better understanding of the nature of the transitions, the frozen solutions were subjected to oscillatory DSC studies (data not presented). This is an extension of conventional DSC in which a sine-wave modulation of the temperature is superimposed on the underlying heating rate. Using mathematical deconvolution, the resultant heat flow can be separated into its heat capacity, or reversible heat flow, and kinetic, or nonreversible heat flow, components (17). This feature was utilized to study reversible events such as glass transition and irreversible events such as enthalpic relaxations and crystallization. For the oscillatory DSC studies, the solutions were cooled from room temperature to –50°C at 20°C/min. Then the DSC module was switched to the oscillatory mode, and the solutions were heated from –50°C to 20°C with a period of 120 sec, an amplitude of ±3°C, and an underlying heating rate of 1°C/min. The crystallization event, as expected, was observed in the nonreversible curve. The glass transition events appeared in the reversible curve. No enthalpic recovery seemed to be associated with the glass transitions.

The frozen aqueous solution literature abounds with examples of two glass transition events. In an effort to understand the significance of the two transitions, a number of theories have been proposed. Many reports have attributed the lower temperature transition to be the true glass transition (19–21). The higher temperature transition has been attributed to an interfacial interaction between ice crystals and the amorphous phase, and has been referred to as "ante" or "incipient" melting (18). Ablett *et al.* (20) and Izzard *et al.* (21) concluded that the higher temperature transition was due to the onset of ice melting. Alternate theories have attributed the higher temperature transition to glass transition of the maximally freeze-concentrated solute (21–23) or to a change in mechanical characteristics referred to as a softening phenomenon (23). The annealing of frozen sucrose solutions resulted in an increase in the lower transition temperature, suggesting that this was the glass transition of a phase plasticized by a higher-than-equilibrium amount of unfrozen water (24).

The effect of the heating rate, ranging from 2°C to 10°C/min was investigated next. Glass transition temperatures usually are affected by heating rate. It was observed that both of the transition temperatures (Tg'_1 and Tg'_2) were influenced by the heating rate (data not shown). Interestingly, the Tg'_2 was not observed at the slowest heating rate, and there seemed to be one continuous transition encompassing both the Tg'_1 and the Tg'_2.

The next series of experiments was designed to ascertain the reversibility of the two transitions. Aqueous mannitol solutions were cooled from room temperature to –50°C at 20°C/min and were held for 20 min. The solutions were heated to temperatures ranging from –26.0 to –23.5°C, were cooled back to –60°C, and were reheated. As the temperature to which the sample was heated in the intermediate scan increased, the following observations were made. (1) There was a progressive decrease in the enthalpy of crystallization. (2) It became increasingly difficult to detect Tg'_2. The decrease in the enthalpy of crystallization strongly suggests crystallization of mannitol during the intermediate heating scan. The decrease in the fraction of the amorphous phase made the detection of Tg'_2 increasingly difficult and prevented an unambiguous interpretation of the results.

Our results indicate that the thermal behavior of aqueous solutions of mannitol, like many other sugars, is characterized by two glass transitions. The interpretation of the DSC curves is complicated by the overlap of the second transition (Tg'_2) with the crystallization exotherm. As a result of the rapid onset of crystallization, there seems to be an endotherm associated with the second transition. We believe that this is an experimental artifact.

When frozen mannitol solutions were heated, the two glass transition events were followed by the crystallization of mannitol (Fig. 3). The very rapid crystallization can be due to the high molecular mobility of the amorphous freeze-concentrate above the glass transition temperatures. Because the solution had been cooled to –50°C at 20°C/min, there was negligible if any crystallization of mannitol during cooling. Solutions also were cooled to –50°C at slower rates of 1°C, 5°C, or 10°C/min. The DSC heating curves of these solutions were qualitatively similar to Fig. 3. The occurrence of the crystallization exotherm indicates that, at all these cooling rates, there was only partial crystallization of mannitol during cooling. Moreover, the presence and the concentration of crystalline mannitol did not seem have any impact on the temperatures of the various thermal events. This suggests that, irrespective of the cooling rate employed, an amorphous freeze-concentrate of mannitol of constant composition is obtained.

Low-temperature XRD was used to ascertain the solid state of mannitol in frozen solutions. The mannitol solution was first cooled to –50°C. The solution then was heated, and XRD patterns were obtained at different temperatures (Fig. 4). However, the solutions were maintained under isothermal conditions during the XRD run. All the peaks observed at –50°C can be attributed to ice. There is no evidence of solute crystallization at this temperature. However, at temperatures $\geq$ –25°C, several new peaks were observed, and, based on the peak positions, the crystallizing solute was identified as mannitol hydrate (10,11). Interestingly, the first evidence of solute crystallization was seen at –35°C. Annealing at temperatures close to the glass transition temperature has been shown to result in the crystallization of solutes such as indomethacin (25). As mentioned earlier, the samples were maintained isothermally during the XRD run. This isothermal hold could be causing the mannitol crystallization. Mannitol solutions with the initial solute concentration ranging from 5% to 12.5% (w/v) were subjected to similar studies, wherein cooling rates of 5°C, 10°C, and 20°C/min were used. The mannitol phase crystallizing from solution was independent of the initial solute concentration as well as the cooling rate.

Mannitol-Phosphate Buffer Salts

We had earlier demonstrated that potassium phosphate buffer salts inhibited the crystallization of mannitol during cooling. The influence of buffer salts, at concentrations of 50, 100, and 150 mM, on the crystallization of mannitol during heating was determined (Fig. 5). At a 50 mM concentration, the DSC curve was substantially similar to that of the frozen aqueous solution of mannitol shown in Fig. 3. In addition to the two glass transitions (events (ii) and (iii) in Fig. 5) and the crystallization (event (iv) in Fig. 5), a small exotherm was

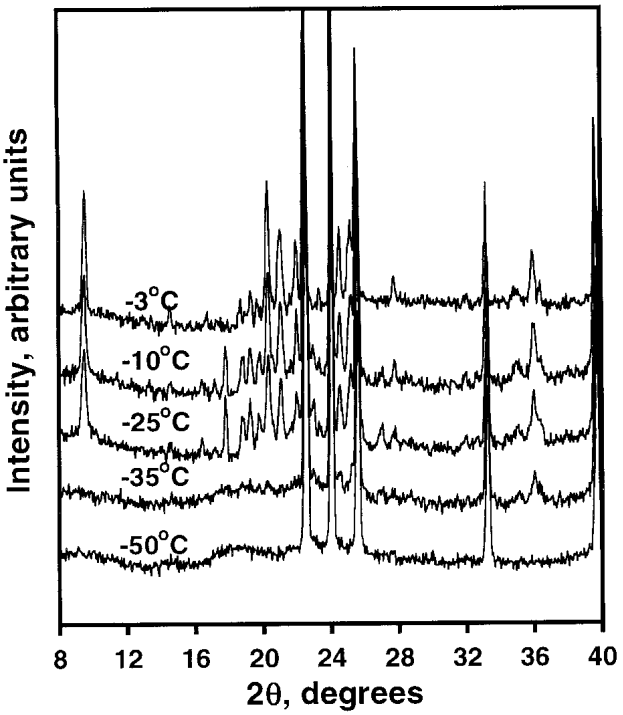

Fig. 4. Variable temperature XRD of frozen mannitol (15% w/w) solution. XRD patterns were obtained at the temperatures indicated in the figure. The solution was initially cooled from room temperature to –50°C at 20°C/min.

observed at –38°C (event (i) in Fig. 5). This may be attributed to the crystallization of one of the buffer salts. Pronounced changes in the DSC curves were observed, when the buffer salt concentrations were increased to 100 or 150 mM. The higher temperature glass transition (event (iii) in Fig. 5) was no longer readily discernible. Moreover, mannitol crystallization was delayed (event (v) in Fig. 5), and there was a pronounced decrease in the enthalpy of crystallization. Thus, at concentrations of 100 and 150 mM, the buffer salts inhibited mannitol crystallization. Although the mechanism of inhibition is not known, the buffer salts may be having an effect on the nucleation.

These solutions also were subjected to XRD. The solutions were first cooled to –50°C and then were heated. The XRD patterns were obtained at different temperatures, as in Fig. 4. Phosphate buffer salts did not significantly inhibit mannitol crystallization during heating (data not shown). The crystallizing phase was identified as mannitol hydrate. This discrepancy between DSC and XRD is possibly due to annealing effects during the XRD analysis. We had earlier pointed out that frozen solutions are maintained under isothermal conditions during the XRD run. The isothermal hold (annealing) could be causing mannitol crystallization. Moreover, the buffer salts did not influence the mannitol phase crystallizing from solution.

Mannitol-PVP Solutions

The DSC heating curves of frozen solutions of mannitol, in the presence of PVP, are shown in Fig. 6. At a low PVP concentration of 0.45% (w/v), the DSC curve was substantially similar to that of the frozen aqueous solution of mannitol shown in Fig. 3. As the PVP concentration was increased, the crystallization exotherm was shifted to higher temperatures, reflecting a delay in the crystallization of mannitol. XRD revealed the crystallization of mannitol hydrate.

SUMMARY AND CONCLUSIONS

There is extensive literature on the solid phases of mannitol, and these reports have been comprehensively summarized by Burger *et al.* (7). Similarly, the physical characterization of freeze-dried mannitol has been the subject of several studies (6,10,11). In this investigation, we have focused on the crystallization behavior of mannitol during the cooling of

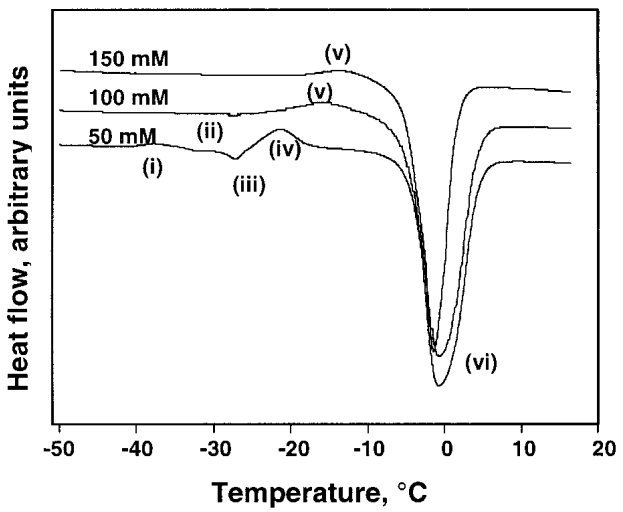

Fig. 5. DSC heating curves of frozen aqueous mannitol (10% w/w) solutions in the presence of potassium phosphate buffer salts. The concentration of the buffer salts ranged from 50 to 150 mM. The solutions were heated from –50°C to 20°C at 10°C/min. The solutions were initially cooled from room temperature to –50°C at 10°C/min.

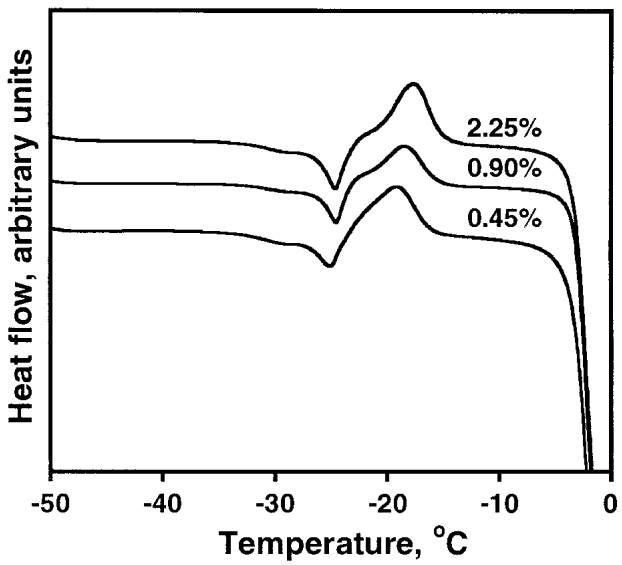

Fig. 6. DSC heating curves of frozen aqueous mannitol (10% w/w) solutions in the presence of PVP. The PVP concentration ranged from 0.45% to 2.25% (w/v). The solutions were heated from –50°C to 20°C at 10°C/min. The solutions were initially cooled from room temperature to –50°C at 10°C/min.

aqueous mannitol solutions and also when the frozen solutions were heated past the glass transition temperatures.

The cooling rate had a significant impact on mannitol crystallization. At the cooling rates investigated, there was partial to complete inhibition of mannitol crystallization. The amorphous freeze-concentrate was characterized by two glass transition temperatures. Heating above the glass transition temperatures resulted in the rapid crystallization of mannitol.

Potassium phosphate buffer salts inhibited mannitol crystallization during the cooling as well as the heating cycle. PVP, at high concentrations, inhibited mannitol crystallization during the cooling cycle, but not during the heating cycle. However, the annealing of all these solutions caused mannitol crystallization. Given the propensity of mannitol to crystallize, we conclude that it is difficult to inhibit the crystallization of mannitol.

Low-temperature XRD, an excellent complement to DSC, enabled the identification of the crystallizing phase as mannitol hydrate. Interestingly, XRD also revealed that mannitol can crystallize when annealed below the glass transition temperatures.

An in-depth evaluation of the crystallization of mannitol below the glass transition temperatures, including the effect of annealing conditions on the crystallization kinetics, will be the subjects of a follow-up report.

ACKNOWLEDGMENTS

Partial financial support from Rhone Poulenc Rorer (now Aventis Pharmaceuticals) is greatly appreciated. We thank Mr. Rahul Surana and Dr. Alan Mackenzie for their valuable comments.

REFERENCES

1. M. J. Pikal. Freeze-drying of proteins: Part I. Process design. *Biopharm.* **3**:18–28 (1990).
2. E. Y. Shalaev and F. Franks. Changes in the physical state of model mixtures during freezing and drying: Impact on product quality. *Cryobiology* **33**:14–26 (1996).
3. J. F. Carpenter, M. J. Pikal, B. S. Chang, and T. W. Randolph. Rational design of stable lyophilized protein formulations: Some practical advice. *Pharm. Res.* **14**:969–975 (1997).
4. J. F. Carpenter and J. H. Crowe. An infrared spectroscopic study of the interactions of carbohydrates with dried proteins. *Biochemistry* **28**:3916–3922 (1989).
5. K. Izutsu, S. Yoshioka, and T. Terao. Effect of mannitol crystallinity on the stabilization of enzymes during freeze-drying. *Chem. Pharm. Bull.* **42**:5–8 (1994).
6. A. I. Kim, M. J. Akers, and S. L. Nail. The physical state of mannitol after freeze-drying: Effects of mannitol concentration, freezing rate, and a noncrystallizing cosolute. *J. Pharm. Sci.* **87**: 931–935 (1998).
7. A. Burger, J. O. Henck, S. Hetz, J. M. Rollinger, A. A. Weissnicht, and H. Stottner. Energy/temperature diagram and compression behavior of the polymorphs of D-mannitol. *J. Pharm. Sci.* **89**:457–468 (2000).
8. L. Yu, D. S. Mishra, and D. R. Rigsbee. Determination of the glass properties of D-mannitol using sorbitol as an impurity. *J. Pharm. Sci.* **87**:774–777 (1998).
9. N. Murase and F. Franks. Salt precipitation during freeze-concentration of phosphate buffer solutions. *Biophys. Chem.* **34**: 293–300 (1989).
10. L. Yu, N. Milton, E. G. Groleau, D. S. Mishra, and R. E. Vansickle. Existence of a mannitol hydrate during freeze-drying and practical implications. *J. Pharm. Sci.* **88**:196–198 (1999).
11. R. K. Cavatur and R. Suryanarayanan. Characterization of phase transitions during freeze-drying by *in situ* X-ray powder diffractometry. *Pharm. Dev. Technol.* **3**:579–586 (1998).
12. K.A. Pikal, and J.F. Carpenter. pH changes during freezing in sodium and potassium phosphate buffer systems in the presence of glycine: Effect on protein stability. *PharmSci Suppl* **1**:S-544 (1998).
13. M. Yoshioka, B. C. Hancock, and G. Zografi. Inhibition of indomethacin crystallization in poly(vinylpyrrolidone) coprecipitates. *J. Pharm. Sci.* **84**:983–986 (1995).
14. G. Van den Mooter, M. Wuyts, N. Blaton, R. Busson, P. Grobet, P. Augustijns, and R. Kinget. Physical stabilization of amorphous ketoconazole in solid dispersions with polyvinylpyrrolidone K25. *Eur. J. Pharm. Sci.* **12**:261–269 (2001).
15. T. Matsumoto and G. Zografi. Physical properties of solid molecular dispersions of indomethacin with poly(vinylpyrrolidone) and poly(vinylpyrrolidone-co-vinylacetate) in relation to indomethacin crystallization. *Pharm. Res.* **16**:1722–1728 (1999).
16. A. Martini, S. Kume, M. Crivellente, and R. Artico. Use of subambient differential scanning calorimetry to monitor the frozen-state behavior of blends of excipients for freeze-drying. *PDA J. Pharm. Sci. Technol.* **51**:62–67 (1997).
17. M. Reading, A. Luget, and R. Wilson. Modulated differential scanning calorimetry. *Thermochim. Acta* **238**:295–307 (1994).
18. B. Luyet and D. Rasmussen. Study by differential thermal analysis of the temperature of instability of rapidly cooled solutions of glycerol, ethylene glycol, sucrose and glucose. *Biodynamica* **10**: 1167–1191 (1968).
19. M. L. LeMeste and D. Simatos. Use of electron spin resonance for the study of "ante-melting" phenomenon observed in sugar solution by differential scanning calorimetry. *Cryo Lett.* **9**:21–63 (1980).
20. S. Ablett, M. J. Izzard, and P. J. Lillford. Differential scanning calorimetric study of frozen sucrose and glycerol solutions. *J. Chem. Soc. Faraday Trans.* **88**:789–794 (1992).
21. M. J. Izzard, S. Ablett, P. J. Lillford, V. L. Hill, and I. F. Groves. A modulated differential scanning calorimetric study: Glass transitions occurring in sucrose solutions. *J. Therm. Anal.* **47**:1407–1418 (1996).
22. H. Levine and L. Slade. Thermomechanical properties of small-carbohydrate-water glasses and "rubbers": Kinetically metastable systems at sub-zero temperatures. *J. Chem. Soc. Faraday Trans.* **84**:2619–2633 (1988).
23. E. Y. Shalaev and F. Franks. Structural glass transitions and thermophysical processes in amorphous carbohydrates and their super-saturated solutions. *J. Chem. Soc. Faraday Trans.* **91**:1511–1517 (1995).
24. L. Chang, X. Tang, M. J. Pikal, N. Milton, and L. Thomas. The origin of multiple glass transitions in frozen aqueous solutions. *Proc. NATAS Annu. Conf. Therm. Anal. Appl.* **27**:624–628 (1999).
25. M. Yoshioka, B. C. Hancock, and G. Zografi. Crystallization of indomethacin from the amorphous state below and above its glass transition temperature. *J. Pharm. Sci.* **83**:1700–1705 (1994).
26. A. Pyne, R. Surana, and R. Suryanarayanan. Crystallization of mannitol below Tg′ during freeze-drying in binary and ternary aqueous systems. *Pharm. Res.* **19**:901–908 (2002).